International Journal of Nanomedicine

Dovepress
open access to scientific and medical research

Open Access Full Text Article

ORIGINAL RESEARCH

Characterization, optimization, and in vitro evaluation of Technetium-99m-labeled niosomes

This article was published in the following Dove Medical Press journal:
International Journal of Nanomedicine

Leanne De Silva[1]
Ju-Yen Fu[2]
Thet Thet Htar[1]
Saravanan Muniyandy[3]
Azahari Kasbollah[4]
Wan Hamirul Bahrin Wan Kamal[4]
Lay-Hong Chuah[1,5]

[1]School of Pharmacy, Monash University Malaysia, Bandar Sunway, Selangor, Malaysia; [2]Nutrition Unit, Malaysian Palm Oil Board, Bandar Baru Bangi, Selangor, Malaysia; [3]Department of Pharmacy, Fatima College of Health Sciences, Al Ain, United Arab Emirates; [4]Medical Technology Division, Malaysian Nuclear Agency, Bangi, Selangor, Malaysia; [5]Advanced Engineering Platform, Monash University Malaysia, Bandar Sunway, Selangor, Malaysia

Background and purpose: Niosomes are nonionic surfactant-based vesicles that exhibit certain unique features which make them favorable nanocarriers for sustained drug delivery in cancer therapy. Biodistribution studies are critical in assessing if a nanocarrier system has preferential accumulation in a tumor by enhanced permeability and retention effect. Radiolabeling of nanocarriers with radioisotopes such as Technetium-99m (^{99m}Tc) will allow for the tracking of the nanocarrier noninvasively via nuclear imaging. The purpose of this study was to formulate, characterize, and optimize ^{99m}Tc-labeled niosomes.

Methods: Niosomes were prepared from a mixture of sorbitan monostearate 60, cholesterol, and synthesized D-α-tocopherol polyethylene glycol 1000 succinate-diethylenetriaminepentaacetic acid (synthesis confirmed by ^{1}H and ^{13}C nuclear magnetic resonance spectroscopy). Niosomes were radiolabeled by surface chelation with reduced ^{99m}Tc. Parameters affecting the radiolabeling efficiency such as concentration of stannous chloride ($SnCl_2 \cdot H_2O$), pH, and incubation time were evaluated. In vitro stability of radiolabeled niosomes was studied in 0.9% saline and human serum at 37°C for up to 8 hours.

Results: Niosomes had an average particle size of 110.2±0.7 nm, polydispersity index of 0.229±0.008, and zeta potential of –64.8±1.2 mV. Experimental data revealed that 30 µg/mL of $SnCl_2 \cdot H_2O$ was the optimal concentration of reducing agent required for the radiolabeling process. The pH and incubation time required to obtain high radiolabeling efficiency was pH 5 and 15 minutes, respectively. ^{99m}Tc-labeled niosomes exhibited high radiolabeling efficiency (>90%) and showed good in vitro stability for up to 8 hours.

Conclusion: To our knowledge, this is the first study published on the surface chelation of niosomes with ^{99m}Tc. The formulated ^{99m}Tc-labeled niosomes possessed high radiolabeling efficacy, good stability in vitro, and show good promise for potential use in nuclear imaging in the future.

Keywords: nanotechnology, nanocarriers, radiolabeling, drug delivery, formulation, nuclear imaging

Introduction

Nanotechnology has emerged as a promising approach in nano-medicine with the development of nanocarriers for cancer therapy as one of its main applications.[1] Conventional chemotherapeutics are distributed systemically and can affect both cancer and healthy cells, potentially causing severe side effects. Nanocarriers on the other hand, can be designed in a way that leads to selective targeting and drug delivery to tumors avoiding drug disposition in healthy tissues. Nanocarriers can also be used for controlled drug release or for protection of free drug against premature degradation.[1]

Niosomes are nano-sized vesicles comprised of a closed bilayer structure formed from nonionic surfactants in an aqueous system.[1] Similar to well-established liposomes, niosomes are able to partition hydrophobic drugs into their hydrophobic domains while

Correspondence: Lay-Hong Chuah
School of Pharmacy, Monash University Malaysia, Jalan Lagoon Selatan, Bandar Sunway, 47500 Subang Jaya, Selangor, Malaysia
Tel +60 35 514 4454
Email alice.chuah@monash.edu

Ju-Yen Fu
Nutrition Unit, Malaysian Palm Oil Board, 6, Persiaran Institusi, Bandar Baru Bangi, 43000 Kajang, Selangor, Malaysia
Tel +60 38 769 4592
Email fujuyen@mpob.gov.my

submit your manuscript | www.dovepress.com
Dovepress
http://dx.doi.org/10.2147/IJN.S184912

entrapping hydrophilic substances within their inner aqueous phase. Liposomes in an aqueous system have been shown to have low physical and chemical stability due to problems such as hydrolysis of fatty acid esters and oxidative degradation of unsaturated fatty acids of the phospholipid component.[2–8] Alternatively, niosomes replace chemically unstable phospholipids with nonionic surfactants, which are also easier to handle and store and are more readily available at lower costs.[9–12]

A majority of tumor-targeted nanocarriers rely on passive targeting that can be achieved by exploiting the pathophysiological characteristics of a solid tumor.[13,14] The combination of leaky vasculature and poor lymphatic drainage within the tumor creates a phenomenon known as the enhanced permeability and retention effect within the tumor. This allows nanocarriers within the range of 20–200 nm to gain access to the extravascular space and due to the interstitial fluid flow and the lack of functional lymphatic vessels, these nanocarriers will experience higher retention times in the tumor microenvironment.[13,15,16]

Radiolabeling of nanocarriers enables the tracking of a delivery system through nuclear imaging to determine its accumulation in vivo. Radioisotopes such as Technetium-99m (^{99m}Tc) serve as a useful tool in evaluating biodistribution of nanocarriers noninvasively. ^{99m}Tc has been widely used for the labeling of radiopharmaceuticals, especially, in the field of diagnostics due to its physical and chemical characteristics such as short half-life ($t_{1/2}$6.02 hour), low energy gamma emission (140 keV), and absence of corpuscular radiation, short labeling time (10–30 minute), low cost, and commercial expediency from the Molybdenum-99 (^{99}Mo)/^{99m}Tc generator.[17,18] The short half-life of ^{99m}Tc minimizes the internal radiation hazard allowing for a high intake limit in comparison to other commonly used laboratory radioisotopes.[17]

While the characterization and optimization of radiolabeling efficiency of other vesicular systems such as liposomes with ^{99m}Tc has been extensively investigated and published over the years, to our knowledge there have been no published articles on the surface chelation of ^{99m}Tc-labeled niosomes. On the basis of this consideration, the aim of the present study was to formulate, characterize, and optimize niosomes radiolabeled by surface chelation with ^{99m}Tc suitable for potential use in nuclear imaging.

Material and methods

Materials

D-α-tocopherol polyethylene glycol 1000 succinate (TPGS), 4-dimethylaminopyridine (DMAP), diethylenetriaminepentaacetic acid (DTPA) anhydride, stannous chloride ($SnCl_2 \cdot H_2O$) dihydrate, Sorbitan monostearate (Span) 60, cholesterol, PBS, and pyridine were purchased from Sigma-Aldrich (St Louis, MO, USA). Dimethyl sulfoxide (DMSO) and human serum were obtained from Merck Millipore (Billerica, MA, USA). Dialysis tubing (molecular weight cut-off 1000 Da) was purchased from Spectrum Labs (San Francisco, CA, USA). Sodium bicarbonate ($NaHCO_3$), sodium hydroxide (NaOH), and hydrochloric acid (HCl) were obtained from Systerms ChemAR (Shah Alam, Malaysia). Sephadex G-25 column was purchased from GE Healthcare Bio-Sciences Corp. (Piscataway, NJ, USA). Instant thin layer chromatography (ITLC) silica gel (SG)-coated fiber glass sheet was obtained from Agilent Technologies (Santa Clara, CA, USA). Drytec ^{99m}Tc generator (^{99}Mo activity: 508.4 mCi) was purchased from GE Healthcare UK Ltd. (Little Chalfont, UK).

Synthesis of TPGS-DTPA

In a microwave vial, TPGS (0.5 mmol), DMAP (0.5 mmol), and DTPA anhydride (0.6 mmol) were heated and stirred in DMSO until fully dissolved. The reaction vial was then placed in a microwave synthesizer (CEM Discover S-Class Focused Microwave Synthesis System, Matthews, NC, USA) and heated to 120°C for 1 hour. The mixture was dialyzed (molecular weight cut-off 1000 Da) for 24 hours against distilled water to remove unreacted DTPA and DMAP. The resultant product was obtained by freeze-drying. Yield: 89.3%.

Fourier-transform infrared spectroscopy (FTIR) (attenuated total reflection, cm^{-1}): 1,736 (C=O stretch, ester), 1,650 (C=O stretch carboxylic acid).

^{1}H nuclear magnetic resonance (NMR) (300 MHz, d_6-DMSO): δ 0.80 (s, 3H, CH_3, H-1), 0.83 (s, 3H, CH_3, H-2), 0.84 (s, 3H, CH_3, H-8), 0.85 (s, 3H, CH_3, H-13), 1.05–1.15 (m, 18H, CH_2, [H-4, H-5, H-6, H-9, H-10, H-11, H-14, H-15, H-16]), 1.22 (s, 3H, CH_3, H-17), 1.37–1.52 (m, 3H, CH, H-3, H-7, H-12), 1.74 (m, 2H, CH_2, H-19), 1.89 (s, 3H, CH_3, H-27), 1.92 (s, 3H, CH_3, H-18), 2.00 (s, 3H, CH_3, H-17), 2.54 (m, 2H, CH_2, C-20), 2.69 (t, J=6.9 Hz, 5.7 Hz, 2H, CH_2, H-32), 2.86–2.98 (m, 8H, CH_2, H-40, H-41, H-42, H-43), 2.97 (m, 2H, CH_2, H-31), 3.12 (s, 2H, CH_2, H-39), 3.41–3.51 (m, CH_2, $[H\text{-}36, H\text{-}37]_n$, H-44, H-45, H-46, H-47), 3.61 (m, 2H, CH_2, H-34), 4.14 (m, 2H, CH_2, H-35).

^{13}C NMR (75 MHz, d_6-DMSO): δ 10.92 (CH_3, C-28), 11.21 (CH_3, C-27), 12.06 (CH_3, C-29), 18.93–18.99 (CH_2, C-20), 19.35–19.75 (CH_3, C-8, C-13), 21.85–21.93 (CH_2, C-5, C10, C-15), 23.18 (CH_3, C-1, C-2), 23.61 (CH_3, C-17), 26.82 (CH, C-3), 27.71 (CH_2, C-31), 27.96 (CH_2, C-32), 30.13 (CH_2, C-19), 31.38–31.45 (CH, C-7, C-12), 36.06–36.21 (CH_2, C-6, C-9, C-11), 38.60 (CH_2, C-4, C-14), 39.17 (CH_2, C-16), 49.35 (CH_2, C41, C42), 51.16 (CH_2, C40, C43), 53.81

(CH_2, C39), 54.23 (CH_2, C44, C46, C47), 55.01 (CH_2, C45), 63.00 (CH_2, C-37), 67.67 (CH_2, C-34), 69.23 (CH_2, C-35), 71.78 (CH_2, C36), 74.11 (CH_2, C18), 116.64 (C-21), 121.16 (C-22), 124.36 (C-25), 125.79 (C-24), 139.70 (C-23), 148.00 (C-26), 170.14 (C-33), 170.36 (C-38), 171.40 (C-30), 172.03 (C-48, C-49, C-51), 172.11 (C-50).

Preparation of niosomes

The niosomes were formulated with slight modifications based on a published method by Fu et al.[19] They were prepared by simple sonication method by first stirring a mixture of Span 60 (0.075 M), cholesterol (0.075 M), and synthesized TPGS-DTPA (concentration ranging from 0.010 to 0.037 M) in PBS for 1 hour at 60°C. Sonication was performed using a Q125 sonicator (Qsonica L.L.C, Newton, CT, USA; max 125 W) using a probe with a 1/8 (3 mm) replaceable tip. The probe was introduced up to the middle of the dispersion and with the instrument set at 75% of its maximal capacity (measured power 94 W) for 8 minutes. All dispersions were sonicated surrounded by crushed ice to avoid overheating. Excess unbound materials were removed by size exclusion chromatography using Sephadex G-25.

Dynamic light scattering (DLS) and zeta potential

The particle size (nm) and polydispersity index (PDI) of the niosomes were measured by cumulant analysis with DLS using the Zetasizer Nano ZS (Malvern Instruments, Malvern, UK). The analysis was performed using a He-Ne laser (wavelength of 633 nm) and a detector angle of 173° (refractive index =1.33, viscosity =0.8872 cP) at 25°C. Samples were diluted with a dilution factor of 1:1,000 with Milli-Q water before analysis. Size measurements were carried out in triplicate and the data are expressed as mean ± SD (nm).

The zeta potential (mV) of the niosomes was measured using Laser Doppler Electrophoresis, using Zetasizer Nano ZS (Malvern Instruments). Samples were diluted with a dilution factor of 1:1,000 with Milli-Q water before analysis. Zeta potential measurements were carried out in triplicate and the data are expressed as zeta potential ± SD (mV).

Morphological characterization of niosomes

The morphology of the niosomes was characterized using transmission electron microscope ([TEM], LIBRA 120; Carl Zeiss Meditec AG, Jena, Germany) operating at 120 kV. The niosomes were diluted with a dilution factor of 1:10 with Milli-Q water to reduce the concentration of vesicles. A drop of diluted sample was placed on a copper grid and allowed to air-dry at room temperature. The grid was then negatively stained with phosphotungstic acid. Excess liquid was drawn off using filter paper and left to dry in a desiccator. The grid was then mounted in the instrument and photographs were taken at different magnifications.

Radiolabeling of niosomes

The niosomes were radiolabeled with ^{99m}Tc by surface chelation with TPGS-DTPA, with slight modifications based on a published protocol by Richardson et al.[20] ^{99m}Tc-pertechnetate solution (Na $^{99m}TcO_4$) was obtained by elution from a sterile ^{99}Mo/^{99m}Tc generator using 0.9% w/v NaCl solution. Briefly, 1 mL of $^{99m}TcO_4^-$ (2 mCi/mL) was mixed with $SnCl_2{\cdot}H_2O$. The pH was adjusted using 0.5 M $NaHCO_3$ solution or 0.1 M HCl. To that mixture, 1 mL of niosomal suspension was added and left to stand at room temperature for 15 minutes.

Radiolabeling efficiency

The percentage of radiolabeling efficiency of the radiolabeled complex was measured using methods described earlier.[21] The radiolabeling efficiency was estimated with ascending ITLC using 1×10 cm SG-coated fiber glass sheets (Agilent Technologies) as the stationary phase. Approximately 2–3 µL of the radiolabeled complex was applied at a point 1 cm from one end of the ITLC-SG strip and allowed to dry at room temperature. The strips were allowed to develop for 8 cm from the point of application in appropriate solvent systems. ITLC was performed using two separate mobile phases:

Mobile phase 1: 0.9% (w/v) saline for the determination of free pertechnetate ($^{99m}TcO_4^-$).

Mobile phase 2: mixture of pyridine:acetic-acid:water (3:5:1.5 v/v) for the determination of reduced/hydrolysed ^{99m}Tc (radiocolloids).

After developing, the strips were dried and cut horizontally into two equal halves and the radioactivity (counts per minute [CPM]) in each segment was determined using an automated well-type gamma ray counter (2470 Wizard^2 Automatic Gamma Counter; PerkinElmer Inc., Waltham, MA, USA).

The radiolabeling efficiency was determined according to the following equation:

$$\text{Radiolabeling efficiency (\%)} = \frac{\text{CPM of } ^{99m}\text{Tc} - \text{labeled niosomes}}{(\text{CPM of } ^{99m}\text{Tc} - \text{labeled niosomes} + ^{99m}TcO_4^- + \text{radiocolloids})} \times 100$$

Effect of $SnCl_2 \cdot H_2O$, pH, and incubation time on radiolabeling efficiency

The effects of amount of $SnCl_2 \cdot H_2O$ and pH on the labeling efficiency of ^{99m}Tc-labeled niosomes were carried out to determine the optimum conditions needed for maximum labeling. Prior to the addition of niosomes to $^{99m}TcO_4^-$, $SnCl_2 \cdot H_2O$ was added at 0.01–0.06 mL (1 mg/mL in 0.1 M NaCl) while pH levels were adjusted from 4 to 8. The radiolabeling efficiencies at varying $SnCl_2 \cdot H_2O$ concentration and pH were measured. The mixture of niosomes and ^{99m}Tc were then incubated for up to 40 minutes. The radiolabeling efficiency was measured at different time points to observe the effect of incubation time.

In vitro stability study of ^{99m}Tc-labeled niosomes

The in vitro stability of the ^{99m}Tc-labeled niosomes was determined using 0.9% (w/v) saline and human serum by ascending ITLC-SG technique. ^{99m}Tc-labeled niosomes (0.1 mL) was mixed with 0.9% saline or human serum (1.9 mL) and incubated at 37°C for up to 8 hours. Samples were drawn at 0, 1, 3, 6, and 8 hours after incubation, and the radiolabeling stability was determined by ITLC and an automated well-type gamma ray counter.

Statistical analysis

All data are reported as mean ± SD. The assessment of statistical significance among the results was carried out by Kruskal–Wallis followed by Dunnett's post hoc test using GraphPad PRISM 7.0 (GraphPad Software, Inc., La Jolla, CA, USA), and $P<0.05$ was considered statistically significant.

Results

Synthesis of TPGS-DTPA

Figure 1 (see Figure S1 for full spectrum) shows the chemical structure of the synthesized TPGS-DTPA. Figure 2 shows the FTIR spectra of DTPA anhydride, TPGS, and TPGS-DTPA. The spectrum of DTPA anhydride showed the characteristic peak of the asymmetric and symmetric carbonyl (C=O) stretch of anhydride at 1,770 cm^{-1}.[22] The band at 1,637 cm^{-1} represents the C=O stretch of carboxylic acid.[23] The absorption

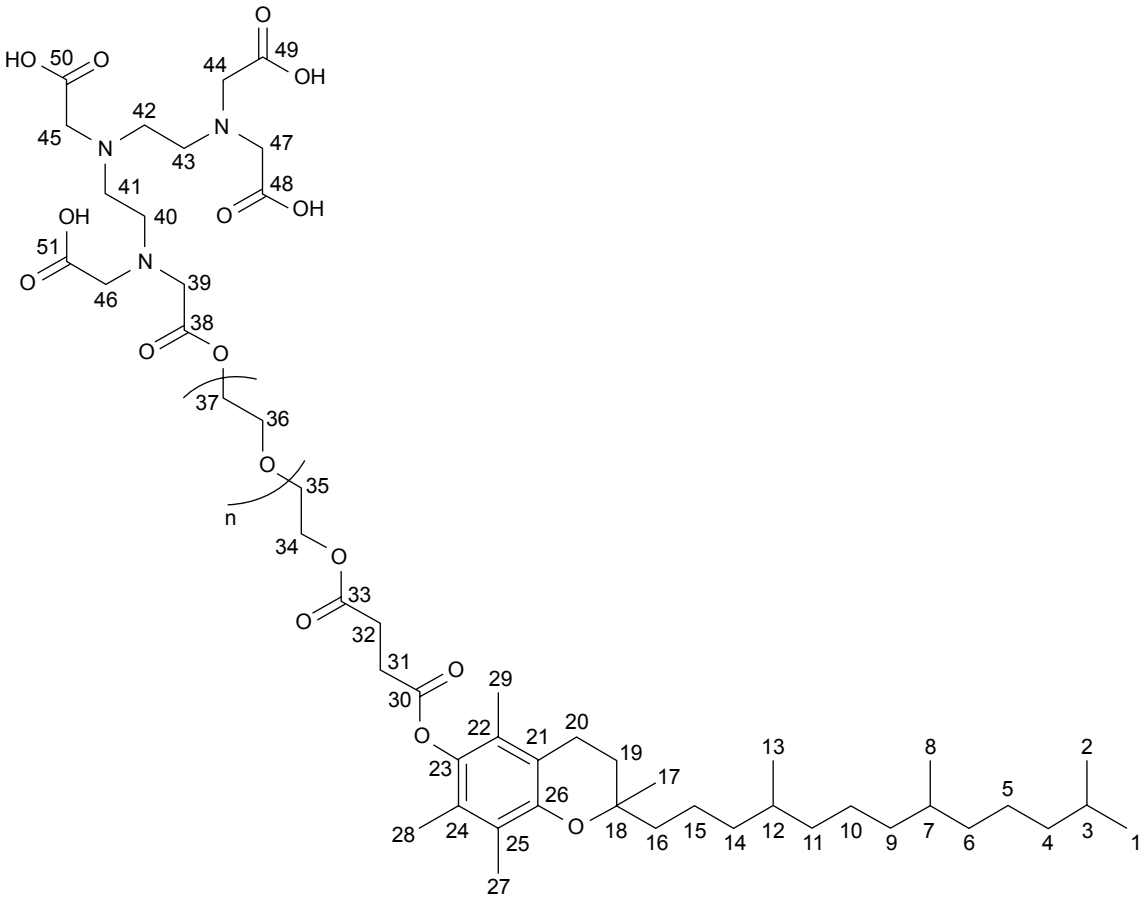

Figure 1 Chemical structure of synthesized TPGS-DTPA.
Abbreviation: TPGS-DTPA, d-α-tocopherol polyethylene glycol 1000 succinate-diethylenetriaminepentaacetic acid.

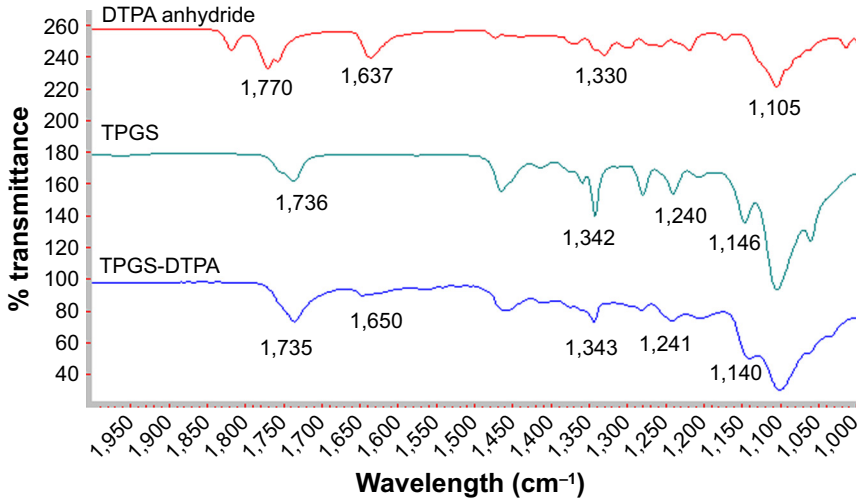

Figure 2 FTIR spectra of DTPA anhydride, TPGS and synthesized TPGS-DTPA.
Abbreviations: DTPA, diethylenetriaminepentaacetic acid; FTIR, Fourier-transform infrared spectroscopy; TPGS, d-α-tocopherol polyethylene glycol 1000 succinate.

peaks of C–O stretch and C–N stretch of DTPA anhydride can be seen at 1,330 and 1,105 cm^{-1} respectively.[22] The peaks of the –C–O–stretching of TPGS can be observed at 1,146 and 1,240 cm^{-1} of the TPGS spectrum.[24] Whereas, the peak for $-CH_2$ group of the polyethylene glycol chain can be observed at 1,342 cm^{-1}. FTIR spectra of synthesized TPGS-DTPA showed an increase in peak intensity at the 1,735 cm^{-1} region proving the occurrence of successful esterification. The appearance of the absorption band 1,650 cm^{-1} representing the carbonyl C=O group of carboxylic acid also further confirmed the conjugation of TPGS to DTPA.

Figure 3 shows the ^{1}H NMR spectra of TPGS and TPGS-DTPA (see Figures S2–S4 for full spectrum) representing the characteristic peaks, which confirmed the formation of

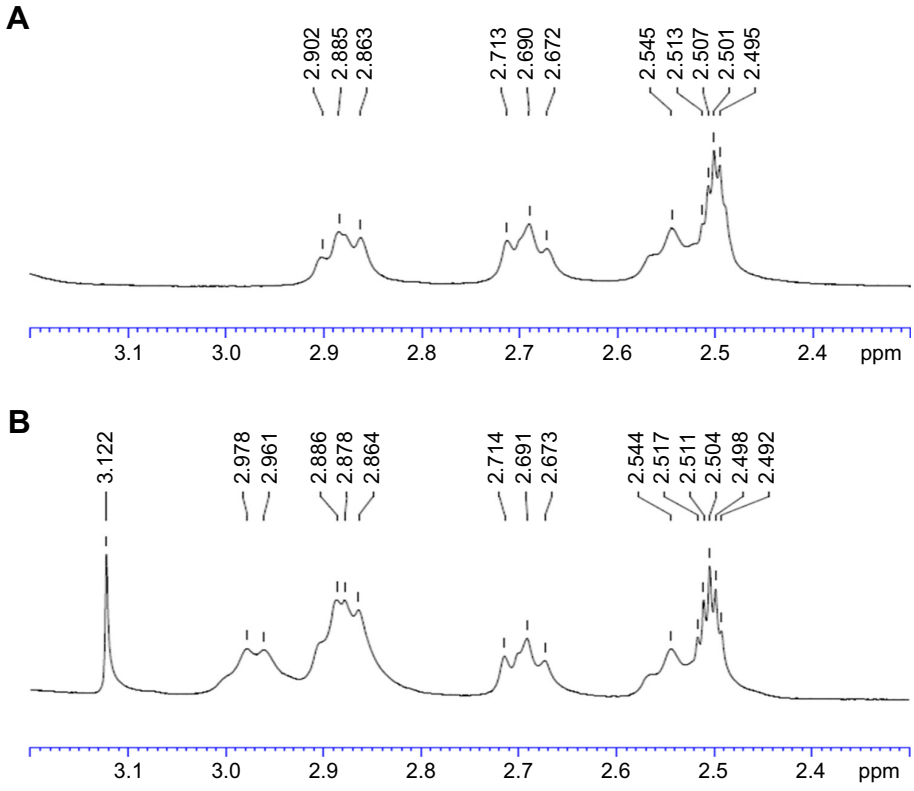

Figure 3 ^{1}H NMR spectra of (**A**) TPGS and (**B**) TPGS-DTPA synthesized via microwave technology.
Abbreviations: DTPA, diethylenetriaminepentaacetic acid; NMR, nuclear magnetic resonance; TPGS, d-α-tocopherol polyethylene glycol 1000 succinate.

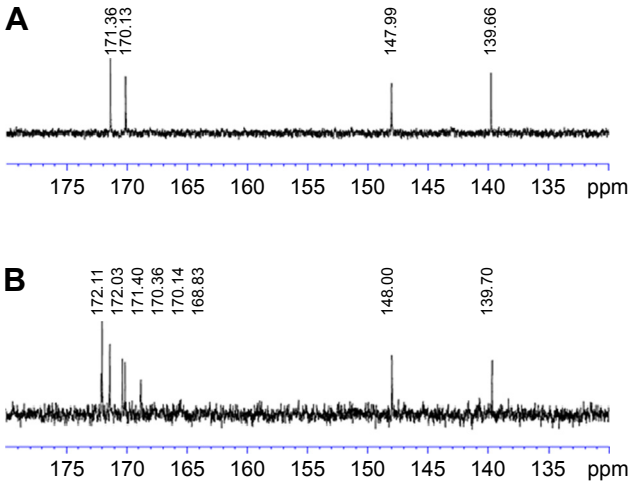

Figure 4 ^{13}C NMR spectra of (**A**) TPGS and (**B**) TPGS-DTPA synthesized via microwave technology.
Abbreviations: DTPA, diethylenetriaminepentaacetic acid; NMR, nuclear magnetic resonance; TPGS, d-α-tocopherol polyethylene glycol 1000 succinate.

TPGS-DTPA. The peak at 3.51 ppm (m) on the TPGS spectra represents the $-CH_2$ protons (C36 and C37) of the polyethylene oxide part of TPGS. The triplet signals at 2.71, 2.69, and 2.67 ppm represent the $-CH_2$ protons (C31) whereas the chemical shifts at 2.98 and 2.96 ppm correspond to the $-CH_2$ (C32). The singlet peaks at 2.00, 1.92, and 1.89 ppm represent the $-CH_3$ (C27–29) of tocopherol aromatic ring. The aforementioned peaks are due to the presence of TPGS in the TPGS-DTPA spectrum. The triplet peaks at 2.89, 2.88, and 2.86 ppm are attributed to the $-CH_2$ (C41 and C42) of DTPA. The additional peak at the chemical shift of 3.12 (s) represents the $-CH_2$ (C39) of DTPA confirming the successful functionalization of DTPA to TPGS.

The ^{13}C NMR spectra in Figure 4 (see Figures S5 and S6 for full spectrum) further confirmed the formation of TPGS-DTPA by presenting the signals of the carboxylic (–COOH) functional group of the DTPA moiety. These signals can be seen at 172.11 (C50) and 172.03 ppm (C49–51). The signal of ester linkage (–C(O)O–) between DTPA and TPGS can also be seen at 171.40 ppm (C38). The additional peaks at 168.8 ppm represent baseline impurities corresponding to the –CH in the aromatic ring of DMAP.

Preparation of niosomes

The preparation of niosomes was straightforward and highly reproducible. Table 1 shows the mean particle size of niosomes formulated with varying concentrations of TPGS-DTPA. The size of the particles ranged from 108.8±2.4 to 173.0±5.9 nm with relatively low PDIs ranging from 0.196±0.023 to 0.308±0.033, indicating relatively good homogeneity of all the dispersions. The particle size results indicate that the incorporation of increasing concentrations of TPGS-DTPA leads to a decrease in size and distribution until the size plateaus at 108.8±1.7 nm (N3), where further increases in TPGS-DTPA concentrations do not result in statistically significant differences in particle size. The niosomes prepared were negatively charged with zeta potential readings ranging from –56.79±5.44 to –69.47±3.41 mV.

The effect of varying concentrations of TPGS-DTPA on radiolabeling efficiency was also evaluated. Table 2 shows that with an increase in concentration of TPGS-DTPA, there was an increase in radiolabeling efficiency from 77.16%±0.87% (N1) to 92.69%±1.84% (N5). The increase in radiolabeling efficiency can be attributed to the decrease in percentage of radiocolloid formation from 17.71%±1.85% (N1) to 1.38%±0.41% (N5) with increasing concentrations of TPGS-DTPA.

Figure 5 shows a TEM micrograph of niosomes (N3) at a magnification of 800×. The niosomes shown were spherical in shape with definite walls. The size of the vesicles obtained ranged from 110.94 to 160.33 nm and were in good agreement with the particle sizes obtained by DLS measurement. Figure 6 shows the image of single niosomes (N3) at a magnification of 25,000×. The observed niosome had a measured particle size of 109.54 nm.

Table 1 Formulation of niosomes (expressed as molar ratio) and their corresponding particle size, PDI, and zeta potential

Formulation	Span 60:cholesterol: TPGS-DTPA	Particle size (nm), mean ± SD	PDI, mean ± SD	Zeta potential, mean ± SD
N1	1:1:0.1	173.0±5.9*	0.232±0.028	–56.8±5.4
N2	1:1:0.2	142.2±6.9*	0.308±0.033	–58.3±2.3
N3	1:1:0.3	108.8±1.7	0.196±0.023	–61.8±2.9
N4	1:1:0.4	109.5±0.8	0.199±0.019	–65.3±4.8
N5	1:1:0.5	108.8±2.4	0.201±0.034	–69.5±3.4

Note: *$P<0.05$, statistically significant (N1, N2, N4, N5 were compared with N3).
Abbreviations: DTPA, diethylenetriaminepentaacetic acid; PDI, polydispersity index; TPGS, d-α-tocopherol polyethylene glycol 1000 succinate.

Table 2 Radiolabeling efficiency of ^{99m}Tc-labeled niosomes with increasing concentrations of TPGS-DTPA

Formulation	$^{99m}TcO_4^-$ (%)	Radiocolloids (%)	^{99m}Tc-labeled niosomes (%)	Loaded amount of ^{99m}Tc (mCi)
N1	5.14±1.15	17.71±1.85	77.16±0.87*	1.54±0.02
N2	5.86±0.47	5.99±1.87	88.15±2.01*	1.76±0.04
N3	5.99±1.95	2.13±0.34	91.88±1.64	1.84±0.03
N4	5.93±1.96	1.38±0.41	92.69±1.84	1.85±0.04
N5	5.85±0.63	1.54±0.36	92.62±0.90	1.85±0.02

Notes: Formulations N1–N5: $SnCl_2 \cdot H_2O$ 30 µg/mL; pH 5; and incubation time 15 min. Data presented as mean ± SD. *$P<0.05$, statistically significant (N1, N2, N4, N5 were compared with N3).
Abbreviations: DTPA, diethylenetriaminepentaacetic acid; $SnCl_2 \cdot H_2O$, stannous chloride; ^{99m}Tc, Technetium-99m; TPGS, d-α-tocopherol polyethylene glycol 1000 succinate.

Radiolabeling of niosomes

The effect of varying the concentration of the reducing agent, $SnCl_2 \cdot H_2O$, on radiolabeling efficiency of niosomes is shown in Table 3. The concentration of $SnCl_2 \cdot H_2O$ added for the reduction of ^{99m}Tc was varied from 10 to 60 µg/mL, keeping the solution at a constant pH 5. The radiolabeling efficiency was 93.50%±0.38% when 10 µg/mL of $SnCl_2 \cdot H_2O$ was added, and it increased significantly to 96.05%±0.26% and 97.38%±0.25% when 20 and 30 µg/mL of $SnCl_2 \cdot H_2O$ was added, respectively. Further increases in $SnCl_2 \cdot H_2O$ concentration resulted in a decrease in percentage of radiolabeling efficiency. The radiolabeling efficiency of ^{99m}Tc-labeled niosomes at different pH levels was also studied (Table 4), keeping the concentration of $SnCl_2 \cdot H_2O$ (30 µg/mL) fixed. As the pH was increased from 4 to 5, an increase in radiolabeling efficiency from 93.90%±0.70% to 96.93%±0.156% was observed. However, further increases in pH to 7 and 8 resulted in the subsequent reduction in radiolabeling efficiency of 92.29%±0.19% and 83.16%±1.31%, respectively. The optimum concentration of $SnCl_2 \cdot H_2O$ and pH for maximum radiolabeling efficiency of ^{99m}Tc-labeled niosomes was determined to be 30 µg/mL and pH 5, respectively.

The effect of incubation time on radiolabeling efficiency was determined, keeping other variables constant including the concentration of $SnCl_2 \cdot H_2O$ and pH at 30 µg/mL and 5, respectively. Figure 7 showed that the formation of ^{99m}Tc-labeled niosomes is dependent on the reaction time. Initially, after a few seconds (corresponding to 0 minute), the radiolabeling efficiency was 92.86%±0.10%. Maximum radiolabeling efficiency was achieved after 15 minutes of incubation time, reaching a maximum radiolabeling efficiency of 97.49%±0.22% and plateaued after 15 minutes.

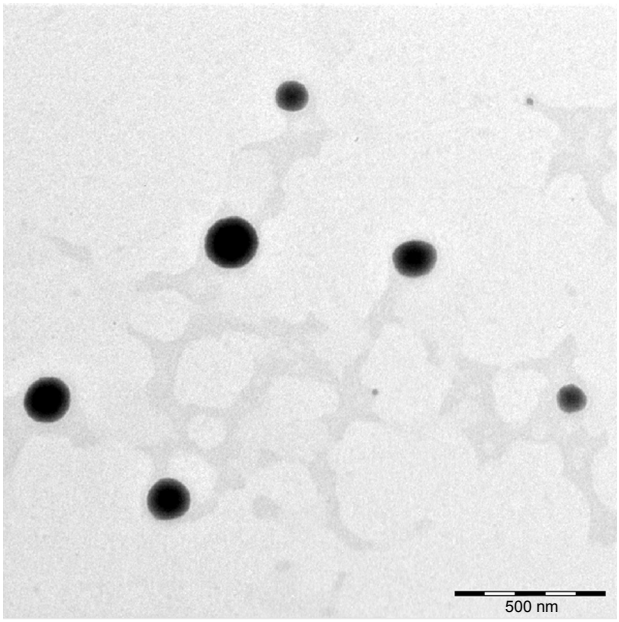

Figure 5 TEM micrograph of niosomes (N3) at a magnification of 800×.
Abbreviation: TEM, transmission electron microscope.

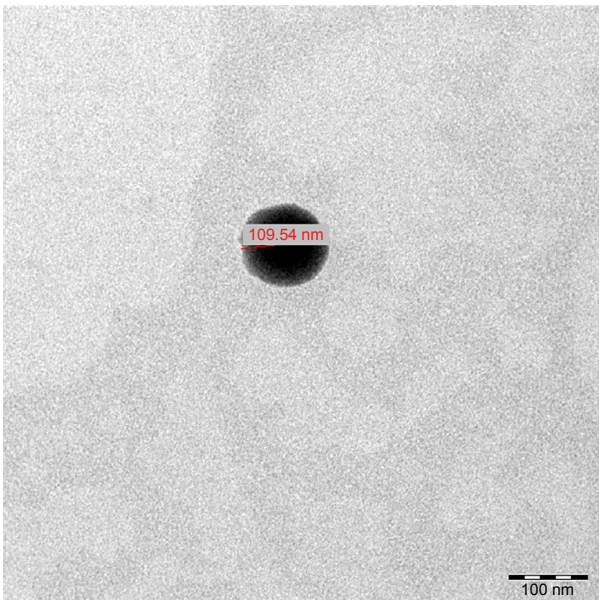

Figure 6 TEM micrograph and measurement of a single niosome (N3) at a magnification of 25,000×.
Abbreviation: TEM, transmission electron microscope.

Table 3 The effect of varying concentrations of $SnCl_2 \cdot H_2O$ on the radiolabeling efficiency of ^{99m}Tc-labeled niosomes (N3)

Concentration of $SnCl_2 \cdot H_2O$ (μg/mL)	$^{99m}TcO_4^-$ (%)	Radiocolloids (%)	^{99m}Tc-labeled niosomes (%)	Loaded amount of ^{99m}Tc (mCi)
10	5.10±0.22	1.39±0.20	93.50±0.38	1.87±0.01
20	2.13±0.27	1.82±0.07	96.05±0.26	1.92±0.01
30	1.59±0.22	1.03±0.04	97.38±0.25	1.95±0.01
40	1.62±0.06	2.28±0.13	96.10±0.15	1.92±0.003
50	1.05±0.20	5.34±0.12	93.61±0.14	1.87±0.002
60	1.17±0.12	7.67±0.30	91.16±0.42	1.82±0.01

Notes: Formulation N3: $SnCl_2 \cdot H_2O$ 10–60 μg/mL; pH 5; and incubation time 15 min. Data presented as mean ± SD.
Abbreviations: $SnCl_2 \cdot H_2O$, stannous chloride; ^{99m}Tc, Technetium-99m.

Therefore, the optimum conditions selected for the radiolabeling of niosomes was 30 μg/mL of $SnCl_2 \cdot H_2O$ at a pH 5 with an incubation time of 15 minutes at room temperature.

The stability of ^{99m}Tc-labeled niosomes was investigated in saline and serum at 37°C (Figure 8). The niosomes showed good in vitro stability with only a 2.48% decrease in radiolabeling efficiency after 8 hours in saline. Comparatively, the niosomes appeared to be less stable in serum, with a loss of radiolabeling efficiency of 14.73% after 8 hours.

Discussion

Synthetic reactions typically involve reaction times ranging from several hours to days at elevated temperatures in order to drive a chemical reaction to completion.[25] In the recent years, organic chemists have turned to microwave-assisted synthesis from conventional heating methods as it can carry out reactions in a shorter time with higher efficiency.[26,27] There is also a reduction in the formation of by-products that are typically generated during the long duration of conventional heating. TPGS is a nonionic, amphiphilic molecule consisting of a lipophilic nonpolar (water-insoluble) head and a hydrophilic (water-soluble) PEG tail. It is formed through the esterification of D-alpha-Tocopheryl acid succinate and PEG 1000.[28–32] DTPA on the other hand, is a commonly used chelating agent that forms coordinate bonds with reduced ^{99m}Tc through the donation of an ion pair of electrons. TPGS was coupled to the carboxylic acid group of DTPA by esterification in a ring-opening reaction to allow for the surface chelation of niosomes with reduced ^{99m}Tc. The reaction resulted in the formation of an ester bond between the hydroxy-terminus of TPGS and the carboxylic group of DTPA. DMAP was added as a catalyst to speed up the rate of reaction and a slight excess of DTPA anhydride was used to ensure that all hydroxy terminals were completely reacted.

Common methods for the preparation of niosomes such as thin-film hydration, ether injection, and reverse phase evaporation require the use of volatile organic solvents.[33,34] Simple sonication method used in this study provides an alternative method to prepare small unilamellar vesicles (SUV) by avoiding the use of harmful organic solvents.[19,35–39] Sonication uses high pressured waves formed from acoustic energy to break up larger multilamellar vesicles and aggregates into SUV.[40] The niosomes were sonicated for a total of 8 minutes. An increase in sonication time resulted in a decrease in particle size and PDI until it reached a plateau (see Table S1).

The physicochemical characteristics of niosomes are critical in determining their success for utilization in vivo. A well-formulated niosomal dispersion should exhibit a

Table 4 The effect of varying pH on the radiolabeling efficiency of ^{99m}Tc-labeled niosomes (N3)

pH	$^{99m}TcO_4^-$ (%)	Radiocolloids (%)	^{99m}Tc-labeled niosomes (%)	Loaded amount of ^{99m}Tc (mCi)
4	3.48±0.18	2.62±0.53	93.90±0.70	1.88±0.02
5	2.38±0.13	0.69±0.15	96.93±0.15	1.93±0.01
6	3.29±0.31	2.48±0.10	94.25±3.31	1.89±0.07
7	4.83±0.07	2.87±0.13	92.29±0.19	1.85±0.01
8	15.81±1.28	1.03±0.09	83.16±1.31	1.66±0.03

Notes: Formulation N3: $SnCl_2 \cdot H_2O$ 30 μg/mL; pH 4–8; and incubation time 15 min. Data presented as mean ± SD.
Abbreviations: $SnCl_2 \cdot H_2O$, stannous chloride; ^{99m}Tc, Technetium-99m.

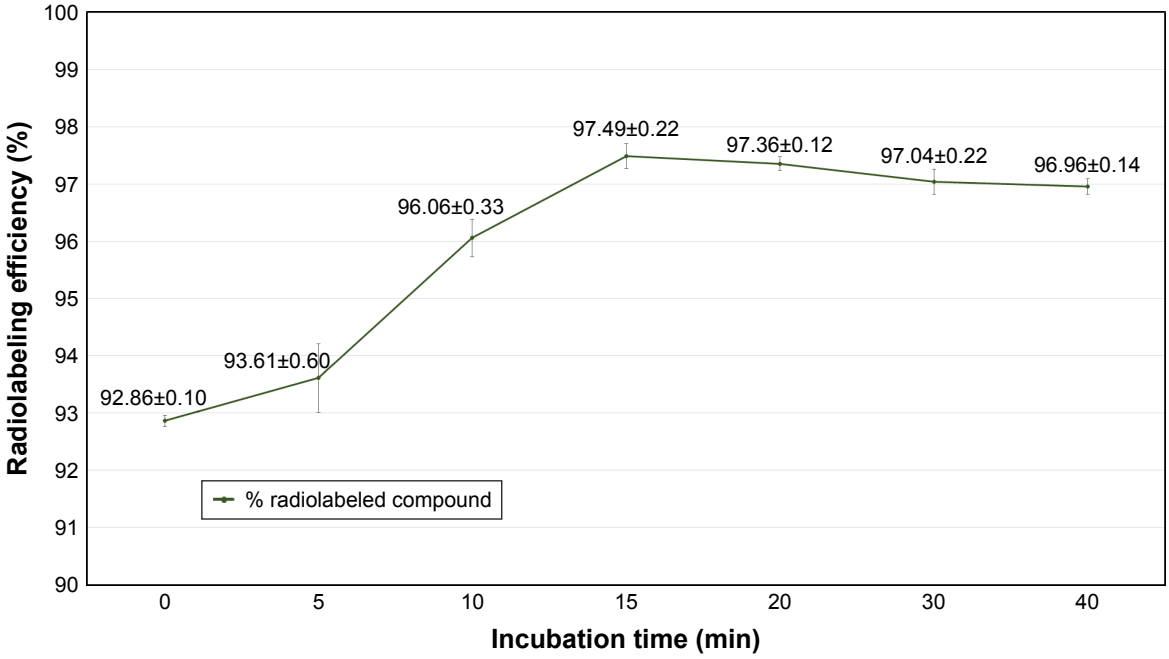

Figure 7 The effect of incubation time on the radiolabeling efficiency of ^{99m}Tc-labeled niosomes (**N3**).
Note: Data presented as mean ± SD.
Abbreviation: ^{99m}Tc, Technetium-99m.

narrow particle size distribution in the nanometer range to be suitable for in vivo injection. It has been reported that to ensure the stability of an injectable colloidal formulation, nanocarriers need to have a mean diameter ≤200 nm.[41] The gradual decrease in particle size of niosomes is attributed to TPGS, which increases the compressibility of the bilayer as a result of dehydration when present in increasing concentrations. This is because TPGS decreases the bilayer defects in the niosomes and enhances the lateral packing of the acyl chains of Span 60, thus resulting in smaller niosomes in size.[42] The PDI value describes the degree of uniformity of a size distribution of particles. PDI values range between

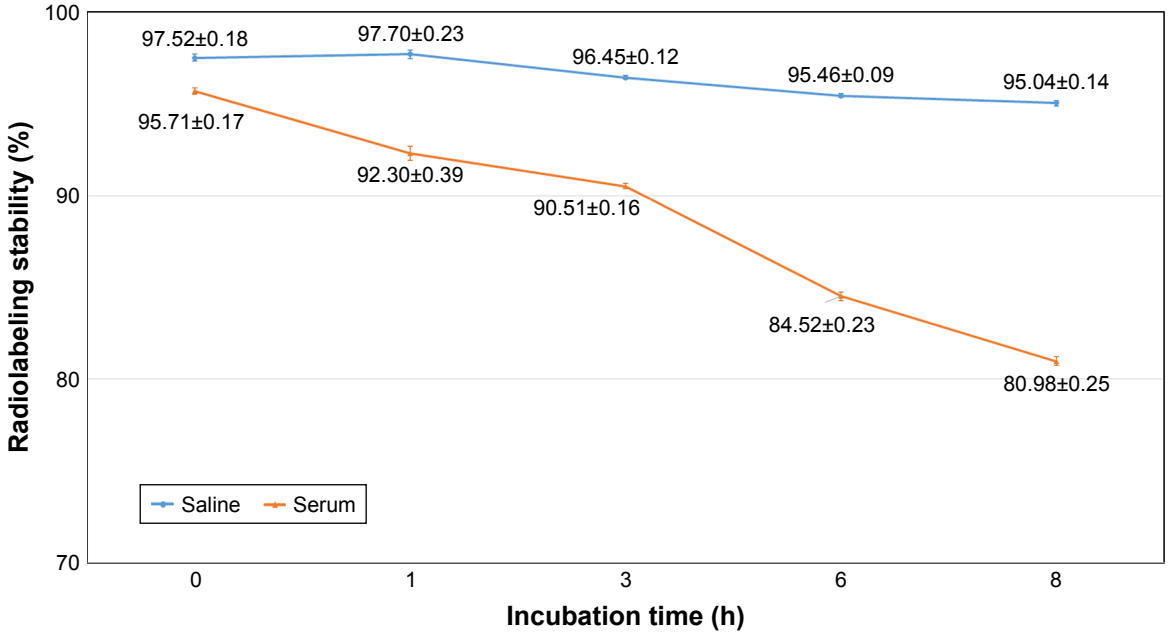

Figure 8 Stability of ^{99m}Tc-labeled niosomes (N3) in saline and serum in vitro at 37°C.
Note: Data presented as mean ± SD. (n= mean ± SD).
Abbreviation: ^{99m}Tc, Technetium-99m.

0.0 (representing a completely monodisperse dispersion) and 1.0 (representing a highly polydisperse dispersion with numerous particle size populations).[43] In the field of drug delivery application for vesicular systems, a PDI of 0.3 and below is typically considered to be acceptable and represents a homogenous dispersion of nanoparticles.[39,44–46] All niosomal formulations exhibited relatively low PDI values, reflecting the particle diameter homogeneity of all dispersions. The increase in TPGS-DTPA concentration also showed a trend with respect to the zeta potential values measured. The decrease in zeta potential value with increasing TPGS-DTPA concentration is attributed to the deprotonation of the free carboxylic groups from DTPA, enhancing the negative charge on the surface of the niosomes. As an indicator of particle surface charge, zeta potential allows for the prediction of the long-term storage stability of a dispersion of colloidal particles.[47] A dispersion is more likely to be stable if it possesses a stronger zeta potential, as charged particles repel each other due to electrostatic repulsion, thereby overcoming their natural tendency to aggregate.[47,48] A study by Crommelin[49] reported that in accordance to the Derjaguin, Landau, Verwey, and Overbeek (DLVO) theory and equation, particles in a dispersion possessing zeta potential of below −30 mV or above +30 mV can reduce particle aggregation by a factor of at least 10^9 in comparison to uncharged particles.[10,48]

^{99m}Tc in the form of pertechnetate ($^{99m}TcO_4^-$) with an oxidation state of +7 is the only ^{99m}Tc compound that is stable in aqueous solution. In this study, $^{99m}TcO_4^-$ was reduced to a lower valency state of +5 using a reducing agent, $SnCl_2{\cdot}H_2O$. The presence of DTPA, a chelating agent on the surface of the niosomes allowed for the immediate chelation of the reduced ^{99m}Tc.[50,51] DTPA is a diethylenetriamine backbone with five carboxymethyl groups. ^{99m}Tc forms a six-coordinate complex with the three nitrogen and three oxygen donor atoms on the DTPA molecule. The major radiochemical impurities generated in radiolabeled compounds are radiocolloids and $^{99m}TcO_4^-$. Radiocolloids typically form as a result of reduction of $^{99m}TcO_4^-$ to ^{99m}Tc with an oxidation state of +4, resulting in the formation of ^{99m}Tc-Sn colloids due to the adsorption of Sn over $^{99m}TcO_2$. Whereas unreacted $^{99m}TcO_4^-$ arises from incomplete reduction due to insufficient addition of $SnCl_2{\cdot}H_2O$ during the radiolabeling process.[50]

The niosomes were labeled with high efficiency (>90%) by surface chelation with reduced ^{99m}Tc. Other authors using similar labeling procedures have also achieved high radiolabeling efficiency yields.[18,21,51] Data on radiolabeling efficiency and stability of the labeled complex were obtained by ITLC using two separate mobile phases. Saline was used as a developing solvent to determine the percentage of $^{99m}TcO_4^-$, which moved with the solvent front (R_f =1.0), while radiocolloids and ^{99m}Tc-labeled niosomes remained at the origin (R_f =0). A separate mobile phase containing pyridine, acetic acid, and water was used to determine the amount of radiocolloids, where radiocolloids remained at the origin (R_f =0) while $^{99m}TcO_4^-$ and ^{99m}Tc-labeled niosomes moved to the solvent front (R_f =1.0). The percentage of radiolabeling efficiency was determined by subtracting the sum of percentage of $^{99m}TcO_4^-$ and radiocolloids from 100%.

The radiolabeling of niosomes was initially conducted both at room temperature (23°C) and at body temperature (37°C). Radiolabeling at room temperature gave rise to similar radiolabeling efficiency (see Table S2). This data aligns with those reported in the literature, where high radiolabeling efficiency can be achieved at room temperature.[52–55] Hence, all radiolabeling processes were conducted at room temperature in this study. The radiolabeling process was optimized by taking four factors into account: concentrations of TPGS-DTPA and $SnCl_2{\cdot}H_2O$, pH of the solution during radiolabeling, and incubation time. The optimum conditions required for maximum radiolabeling efficiency of niosomes were established. Prior to the reduction of $^{99m}TcO_4^-$, $SnCl_2{\cdot}H_2O$ was dissolved in an acid to prevent the hydrolysis of Sn^{2+}.[56] It was determined that niosomes formulated from a molar ratio of Span 60:cholesterol:TPGS-DTPA at 1:1:0.3 (formulation N3) had the optimum concentration of TPGS-DTPA for maximum radiolabeling. The amount of DTPA in the formulation available for complexation during the radiolabeling process is crucial, as an insufficient amount would lead to poor radiolabeling efficiency with a high yield of radiocolloids. Therefore, formulation N3 was chosen as the optimal formulation with respect to the mean particle size (nm), PDI, zeta potential (mV), and radiolabeling efficiency (%) and was used for further radiolabeling studies.

The amount of $SnCl_2{\cdot}H_2O$ added for the reduction of $^{99m}TcO_4^-$ also plays a crucial role in the radiolabeling process. High amounts of $SnCl_2{\cdot}H_2O$ result in the formation of stannous hydroxide colloid impurities, which compete with the complexation process, resulting in reduced complex formation between DTPA and ^{99m}Tc.[51,57] In contrast, insufficient amounts of $SnCl_2{\cdot}H_2O$ result in poor radiolabeling efficiency with a high amount of $^{99m}TcO_4^-$ impurities due to insufficient reductions. Our results showed that 30 µg/mL of $SnCl_2{\cdot}H_2O$ was required for maximum radiolabeling of niosomes. Studies on the effect of pH found that pH 5 was the most suitable pH for the radiolabeling of niosomes.

At lower pH values, $^{99m}TcO_4^-$ with a valency of +7 tends to be reduced to +4, thereby producing more $^{99m}TcO_2$ impurities resulting in a lower radiolabeling efficiency. Similar to literature, there was also a reduction in radiolabeling efficiency with an increase in pH.[58,59] At higher pH, the high concentration of OH^- in the reaction mixture may contribute to the incomplete reduction of ^{99m}Tc and partial hydrolysis of the formed complex, resulting in a low radiolabeling efficiency.[57] The complexation of ^{99m}Tc with TPGS-DTPA was not rapid and required 15 minutes. As the reaction between stannous ions and $^{99m}TcO_4^-$ occurs almost instantaneously and completely, the rate limiting step was the complexation of ^{99m}Tc with DTPA through the formation of a six-coordinate complex. This was not unexpected as there have been previous studies which reported the incubation time required for radiolabeling of particles with ^{99m}Tc typically range from 5 to 15 minutes.[21,57,59]

The in vitro stability of ^{99m}Tc-labeled niosomes was assessed by incubation with 0.9% saline and healthy human serum at body temperature. These conditions were chosen to mimic the applied environment of the ^{99m}Tc-labeled niosomes during in vitro storage and in vivo internal environment and physiological pH. As ^{99m}Tc-pertechnetate solution ($Na\ ^{99m}TcO_4$) is obtained by elution from a $^{99}Mo/^{99m}Tc$ generator using 0.9% (w/v) saline, it is important for ^{99m}Tc-labeled niosomes to remain stable in saline. The ^{99m}Tc-labeled niosomes were found to be extremely stable in saline with only a 2.48% decrease in radiolabeling efficiency after 8 hours. This result was comparable to that obtained by Arulsudar et al[21], who prepared ^{99m}Tc-labeled liposomes by direct labeling for in vivo studies in Ehrlich ascites tumor-bearing mice. Human serum on the other hand, contains a variety of proteins that have the potential to chelate with ^{99m}Tc, therefore affecting the stability of ^{99m}Tc-labeled niosomes in the blood when administered intravenously.[60] As a tumor imaging agent, it is crucial for ^{99m}Tc-labeled niosomes to remain stable during the course of the study to ensure accurate interpretation of the biodistribution and imaging data of niosomes when administered in vivo. The experimental data found that there was little dissociation of ^{99m}Tc from the niosomes after 8 hours, signifying the stability as well as the suitability of ^{99m}Tc-labeled niosomes for in vivo use. The slight reduction in radiolabeling efficiency of the ^{99m}Tc-labeled niosomes after 8 hours could be attributed to the enzymatic degradation of the ester bond between TPGS-DTPA or transchelation of ^{99m}Tc to serum proteins. Comparable in vitro stability of ^{99m}Tc-liposomes prepared by direct labeling was reported by other authors with similar percentage dissociations of ^{99m}Tc at 8 hours.[18,57] This was unexpected as ^{99m}Tc-labeled niosomes labeled by surface chelation were predicted to possess a higher in vitro stability in comparison to direct labeling of liposomes. Direct labeling involves ^{99m}Tc directly forming bonds with the functional groups of the nanocarrier whereas surface chelation involves the chelation of ^{99m}Tc to a lipid-chelator conjugate incorporated in the bilayer.[61] Surface chelation was expected to exhibit a higher stability in vitro in comparison to direct labeling as chelators such as DTPA bind more strongly with ^{99m}Tc.

The aim of this work was to formulate, characterize, and optimize a niosome prototype suitable for use in nuclear imaging. The niosomes could subsequently be loaded with therapeutic agents for various applications. It should be noted that certain properties of the niosomes could be altered once they are loaded with therapeutic agents, and thorough characterization and investigations should be carried out to explore the pharmacokinetics and biodistribution of such system. Though the present study is limited to the data of empty niosomes, we have previously investigated the ability of a similar system to encapsulate therapeutic agents, using hydrophobic tocotrienol (T3) as a model compound, demonstrating the drug encapsulation capacities of the niosomes.[62] T3-loaded niosomes have also been formulated and characterized as a drug model and found to have no significant difference in terms of physical properties from the empty niosomes in terms of particle size and zeta potential (see Table S3). As the biodistribution and pharmacokinetic profile of a nanocarrier is largely dependent on its physicochemical properties such as size and charge, it is expected that the drug-loaded niosomes will behave similarly to the formulated empty niosomes. Published work by Fu et al[19] on T3-loaded niosomes with a similar composition to our system also demonstrated the drug loading capacities of this system.

Conclusion

^{99m}Tc-labeled niosomes as potential nanocarriers for nuclear imaging have been successfully formulated. Surface chelation was chosen as the method to radiolabel niosomes as it has been shown to be more stable in vivo due to the strong affinity of chelating agent, DTPA, for ^{99m}Tc. TPGS-DTPA was successfully synthesized by microwave-assisted technology as confirmed by FTIR and ^1H and ^{13}C NMR. An increase in TPGS-DTPA concentration in the niosomal formulation was found to result in a decrease in particle size, PDI, and zeta potential with an increase in radiolabeling efficiency. The study found that 30 µg/mL $SnCl_2 \cdot H_2O$ was the optimal concentration of reducing agent required for the

radiolabeling process. The optimal pH value and incubation time of the niosomes in terms of labeling efficiency was 5 and 15 minutes, respectively. The ^{99m}Tc-labeled niosomes were found to possess sufficient stability in an in vitro environment for up to 8 hours. The results presented in this study illustrate that ^{99m}Tc-labeled niosomes have appropriate radiolabeling efficiency and stability in vitro and show good promise as potential radiolabeled nanocarriers that can be used for nuclear imaging for future in vivo use.

Acknowledgments

This work was supported by the Fundamental Research Grant Scheme (FRGS), by the Ministry of Higher Education, Malaysia (FRGS/2/2014/SG05/MUSM/03/3), and the Malaysian Palm Oil Board (MPOB).

Disclosure

The authors report no conflicts of interest in this work.

References

1. Williams EC, Toomey R, Alcantar N. Controlled release niosome embedded chitosan system: Effect of crosslink mesh dimensions on drug release. *J Biomed Mater Res A*. 2012;100A(12):3296–3303.
2. Abdelkader H, Alani AW, Alany RG. Recent advances in non-ionic surfactant vesicles (niosomes): self-assembly, fabrication, characterization, drug delivery applications and limitations. *Drug Deliv*. 2014; 21(2):87–100.
3. Marianecci C, di Marzio L, Rinaldi F, et al. Niosomes from 80s to present: the state of the art. *Adv Colloid Interface Sci*. 2014;205:187–206.
4. Fathalla D, Abdel-Mageed A, Abdel-Hamid F, In-Vitro AM. In-vitro and in-vivo evaluation of niosomal gel containing aceclofenac for sustained drug delivery. *Int J Pharm Sci Res*. 2014;1(1):1–11.
5. Vikbjerg AF, Andresen TL, Jørgensen K, Mu H, Xu X. Oxidative stability of liposomes composed of docosahexaenoic acid-containing phospholipids. *J Am Oil Chem Soc*. 2007;84(7):631–637.
6. Grit M, Crommelin DJ. Chemical stability of liposomes: implications for their physical stability. *Chem Phys Lipids*. 1993;64(1–3):3–18.
7. Guldiken B, Gibis M, Boyacioglu D, Capanoglu E, Weiss J. Physical and chemical stability of anthocyanin-rich black carrot extract-loaded liposomes during storage. *Food Res Int*. 2018;108:491–497.
8. Toh M-R, Chiu GNC. Liposomes as sterile preparations and limitations of sterilisation techniques in liposomal manufacturing. *Asian J Pharm*. 2013;8(2):88–95.
9. Manosroi A, Wongtrakul P, Manosroi J, et al. Characterization of vesicles prepared with various non-ionic surfactants mixed with cholesterol. *Colloids and Surfaces B: Biointerfaces*. 2003;30(1–2):129–138.
10. Marianecci C, Rinaldi F, Mastriota M, et al. Anti-inflammatory activity of novel ammonium glycyrrhizinate/niosomes delivery system: human and murine models. *J Control Release*. 2012;164(1):17–25.
11. Riaz M, Riaz M, Zhang X, et al. Surface Functionalization and targeting strategies of liposomes in solid tumor therapy: a review. *Int J Mol Sci*. 2018;19(1):195.
12. Huang Z, Li X, Zhang T. A review on phospholipids and their main applications in drug delivery systems. *Asian J Pharm*. 2014;10(2):81–98.
13. Byrne JD, Betancourt T, Brannon-Peppas L. Active targeting schemes for nanoparticle systems in cancer therapeutics. *Adv Drug Deliv Rev*. 2008;60(15):1615–1626.
14. Leite EA, Lana AM, Junior AD, Coelho LG, de Oliveira MC. Acute toxicity study of cisplatin loaded long-circulating and pH-sensitive liposomes administered in mice. *J Biomed Nanotechnol*. 2012;8(2): 229–239.
15. Golombek SK, May JN, Theek B, et al. Tumor targeting via EPR: strategies to enhance patient responses. *Adv Drug Deliv Rev*. 2018;130:17–38.
16. Haley B, Frenkel E. Nanoparticles for drug delivery in cancer treatment. *Urol Oncology: Seminars and Original Investigations*. 2008; 26(1):57–64.
17. Akbar MU, Ahmad MR, Shaheen A, Mushtaq S. A review on evaluation of technetium-99m labeled radiopharmaceuticals. *J Radioanal Nucl Chem*. 2016;310(2):477–493.
18. de Barros ALB, de Andrade SF, de Souza Filho JD, Cardoso VN, Alves RJ. Radiolabeling of low molecular weight d-galactose-based glycodendrimer with technetium-99m and biodistribution studies. *J Radioanal Nucl Chem*. 2013;298(1):605–609.
19. Fu JY, Zhang W, Blatchford DR, Tetley L, Mcconnell G, Dufès C. Novel tocotrienol-entrapping vesicles can eradicate solid tumors after intravenous administration. *J Control Release*. 2011;154(1):20–26.
20. Richardson VJ, Jeyasingh K, Jewkes RF, Ryman BE, Tattersall MHN. Properties of [^{99m}Tc] Technetium-labelled liposomes in normal and tumour-bearing rats. *Biochem Soc Trans*. 1977;5(1):290–291.
21. Arulsudar N, Subramanian N, Mishra P, Chuttani K, Sharma RK, Murthy RS. Preparation, characterization, and biodistribution study of technetium-99m-labeled leuprolide acetate-loaded liposomes in Ehrlich ascites tumor-bearing mice. *AAPS PharmSci*. 2004;6(1):45–56.
22. Roosen J, Binnemans K. Adsorption and chromatographic separation of rare earths with EDTA- and DTPA-functionalized chitosan biopolymers. *J Mater Chem A*. 2014;2(5):1530–1540.
23. Akhlaghi M, Pourjavadi A. Preparation and primary evaluation of 66Ga-DTPA-chitosan in fibrosarcoma bearing mice Nukleonika. 2011;56(1):41–47.
24. Sonali, Agrawal P, Singh RP, et al. Transferrin receptor-targeted vitamin E TPGS micelles for brain cancer therapy: preparation, characterization and brain distribution in rats. *Drug Deliv*. 2016;23(5):1788–1798.
25. Santagada V, Frecentese F, Perissutti E, Fiorino F, Severino B, Caliendo G. Microwave assisted synthesis: a new technology in drug discovery. *Mini Rev Med Chem*. 2009;9(3):340–358.
26. Mistry B, Medhane D, Mohanraj K, Ghone SA. Microwave-assisted synthesis of an important intermediate of benazepril. *Indian J Pharm Sci*. 2010;72(3):378–380.
27. Porcheddu A, Giacomelli G, Salaris M. Microwave-assisted synthesis of isonitriles: a general simple methodology. *J Org Chem*. 2005;70(6): 2361–2363.
28. Guo Y, Luo J, Tan S, Otieno BO, Zhang Z. The applications of Vitamin E TPGS in drug delivery. *Eur J Pharm Sci*. 2013;49(2):175–186.
29. Muthu MS, Kulkarni SA, Xiong J, Feng SS. Vitamin E TPGS coated liposomes enhanced cellular uptake and cytotoxicity of docetaxel in brain cancer cells. *Int J Pharm*. 2011;421(2):332–340.
30. Huang L, Chen H, Zheng Y, et al. Nanoformulation of D-α-tocopheryl polyethylene glycol 1000 succinate-b-poly(ε-caprolactone-ran-glycolide) diblock copolymer for breast cancer therapy. *Integr Biol (Camb)*. 2011;3(10):993–1002.
31. Collnot EM, Baldes C, Wempe MF, et al. Mechanism of inhibition of P-glycoprotein mediated efflux by vitamin E TPGS: influence on ATPase activity and membrane fluidity. *Mol Pharm*. 2007;4(3):465–474.
32. Muthu MS, Kutty RV, Luo Z, Xie J, Feng SS. Theranostic vitamin E TPGS micelles of transferrin conjugation for targeted co-delivery of docetaxel and ultra bright gold nanoclusters. *Biomaterials*. 2015;39: 234–248.
33. Ag Seleci D, Seleci M, Walter J-G, Stahl F, Scheper T. Niosomes as nanoparticular drug carriers: fundamentals and recent applications. *J Nanomater*. 2016;2016(3):1–13.
34. Asthana GS, Sharma PK, Asthana A. In vitro and in vivo evaluation of niosomal formulation for controlled delivery of clarithromycin. *Scientifica (Cairo)*. 2016;2016:10.
35. Fu JY, Blatchford DR, Tetley L, Dufès C. Tumor regression after systemic administration of tocotrienol entrapped in tumor-targeted vesicles. *J Control Release*. 2009;140(2):95–99.
36. Dufès C, Muller JM, Couet W, Olivier JC, Uchegbu IF, Schätzlein AG. Anticancer drug delivery with transferrin targeted polymeric chitosan vesicles. *Pharm Res*. 2004;21(1):101–107.

37. Yasin MN, Hussain S, Malik F, et al. Preparation and characterization of chloramphenicol niosomes and comparison with chloramphenicol eye drops (0.5%w/v) in experimental conjunctivitis in albino rabbits. *Pak J Pharm Sci*. 2012;25(1):117–121.
38. Kumar YP, Kumar KV, Kishore VS. Preparation and evaluation of diclofenac niosomes by various techniques. *Res J Pharm Tech*. 2013; 6(10):1097–1101.
39. Taladrid D, Marín D, Alemán A, Álvarez-Acero I, Montero P, Gómez-Guillén MC. Effect of chemical composition and sonication procedure on properties of food-grade soy lecithin liposomes with added glycerol. *Food Res Int*. 2017;100(Pt 1):541–550.
40. Cho NJ, Hwang LY, Solandt JJR, Frank CW. Comparison of extruded and sonicated vesicles for planar bilayer self-assembly. *Materials*. 2013;6(8):3294–3308.
41. Monteiro LOF, Fernandes RS, Oda CMR, et al. Paclitaxel-loaded folate-coated long circulating and pH-sensitive liposomes as a potential drug delivery system: a biodistribution study. *Biomed Pharmacother*. 2018;97:489–495.
42. Garbuzenko O, Barenholz Y, Priev A. Effect of grafted PEG on liposome size and on compressibility and packing of lipid bilayer. *Chem Phys Lipids*. 2005;135(2):117–129.
43. Danaei M, Dehghankhold M, Ataei S, et al. Impact of particle size and polydispersity index on the clinical applications of lipidic nanocarrier systems. *Pharmaceutics*. 2018;10(2):57.
44. Badran M. Formulation and in vitro evaluation of flufenamic acid loaded deformable liposomes for improved skin delivery. *Dig J Nanomater Bios*. 2014;9(1):83–91.
45. Chen M, Liu X, Fahr A. Skin penetration and deposition of carboxyfluorescein and temoporfin from different lipid vesicular systems: in vitro study with finite and infinite dosage application. *Int J Pharm*. 2011; 408(1–2):223–234.
46. Kakkar D, Dumoga S, Kumar R, Chuttani K, Mishra AK. PEGylated solid lipid nanoparticles: design, methotrexate loading and biological evaluation in animal models. *Medchemcomm*. 2015;6(8):1452–1463.
47. Hadian Z, Sahari MA, Moghimi HR, Barzegar M. Formulation, characterization and optimization of liposomes containing eicosapentaenoic and docosahexaenoic acids; a methodology approach. *Iran J Pharm Res*. 2014;13(2):393–404.
48. Heurtault B, Saulnier P, Pech B, Proust JE, Benoit JP. Physicochemical stability of colloidal lipid particles. *Biomaterials*. 2003; 24(23):4283–4300.
49. Crommelin DJ. Influence of lipid composition and ionic strength on the physical stability of liposomes. *J Pharm Sci*. 1984;73(11):1559–1563.
50. Majumdar D, Saha CN, Pradesh A. 99mTechnetium radiolabeling and biodistribution studies of some peptide-based ligands. *World J Medical Sciences*. 2011;6(3):105–110.
51. Garg M, Garg BR, Jain S, et al. Radiolabeling, pharmacoscintigraphic evaluation and antiretroviral efficacy of stavudine loaded 99mTc labeled galactosylated liposomes. *Eur J Pharm Sci*. 2008;33(3):271–281.
52. Chen Y, Wen Huang Z, He L, Long Zheng S, Lian Li J, Lian Qin D. Synthesis and evaluation of a technetium-99m-labeled diethylenetriaminepentaacetate–deoxyglucose complex ([99mTc]–DTPA–DG) as a potential imaging modality for tumors. *Appl Radiot Isot*. 2006; 64(3):342–347.
53. Wang J, Yang W, Xue J, Zhang Y, Liu Y. Synthesis, ^{99m}Tc-labeling, and preliminary biological evaluation of DTPA-melphalan conjugates. *J Label Compd Radiopharm*. 2017;60(14):659–665.
54. Altıparmak B, Lambrecht FY, Er O. Design of ^{99m}Tc-DTPA-CLP and preliminary evaluation in rats. *Chem Biol Drug Des*. 2014;83(3):362–366.
55. Kakkar D, Tiwari AK, Chuttani K, Kaul A, Singh H, Mishra AK. Comparative evaluation of glutamate-sensitive radiopharmaceuticals: Technetium-99m–glutamic acid and technetium-99m–diethylenetriaminepentaacetic acid–bis(Glutamate) conjugate for tumor imaging. *Cancer Biother Radiopharm*. 2010;25(6):645–655.
56. Patel A, Tyagi A, Sharma RK, Thakkar H. A gamma scintigraphy study to investigate uterine targeting efficiency of raloxifene-loaded liposomes administered intravaginally in New Zealand white female rabbits. *Drug Deliv Transl Res*. 2016e-pub ahead of print.
57. Eid Moustapha M, Shweeta HA, Motaleb MA. Technetium-labeled danofloxacin complex as a model for infection imaging. *Arab J Chem*. 2016;9(S2):S1928–S1934.
58. Arulsudar N, Subramanian N, Mishra P, Sharma RK, Murthy RS. Preparation, characterisation and biodistribution of 99mTc-labeled liposome encapsulated cyclosporine. *J Drug Target*. 2003;11(3):187–196.
59. Rizvi FA, Bokhari TH, Roohi S, Mushtaq A. Direct labeling of doxorubicin with technetium-99m: its optimization, characterization and quality control. *J Radioanal Nucl Chem*. 2012;293(1):303–307.
60. He Z, Zhang X, Huang J, et al. Immune activity and biodistribution of polypeptide K237 and folic acid conjugated amphiphilic PEG-PLGA copolymer nanoparticles radiolabeled with 99mTc. *Oncotarget*. 2016; 7(47):76635–76646.
61. Fragogeorgi EA, Savina IN, Tsotakos T, et al. Comparative in vitro stability and scintigraphic imaging for trafficking and tumor targeting of a directly and a novel ^{99}mTc(I)$(CO)_3$ labeled liposome. *Int J Pharm*. 2014;465(1–2):333–346.
62. Chuah LH, de Silva L, Saravanan M, Fu JY. Preparation and optimization of tocotrienol rich fraction (TRF)-loaded niosomes. *Asian J Pharm*. 2016;11(1):56–57.

Supplementary materials

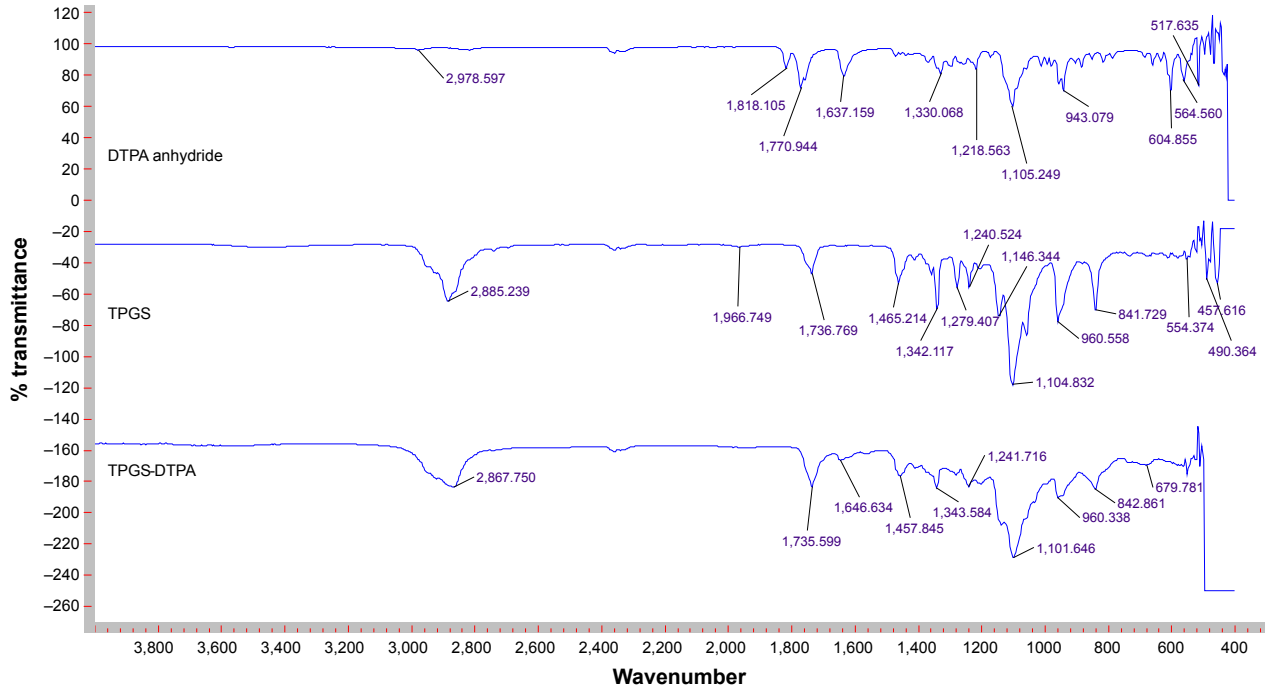

Figure S1 Full range FTIR spectra (400–4,000 cm^{-1}) of DTPA anhydride, TPGS, and synthesized TPGS-DTPA.
Abbreviations: DTPA, diethylenetriaminepentaacetic acid; FTIR, Fourier-transform infrared spectroscopy; TPGS, d-α-tocopherol polyethylene glycol 1000 succinate.

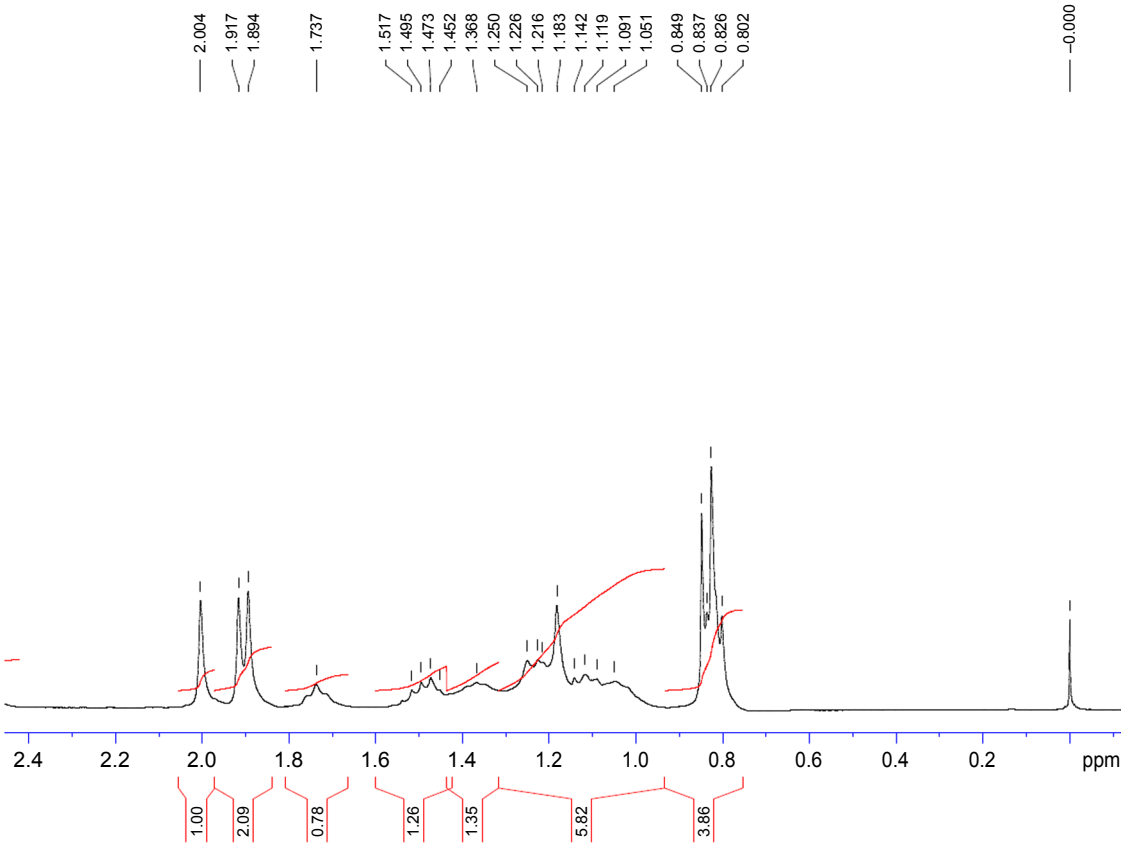

Figure S2 ^1H NMR spectrum (0–2.4 ppm) of TPGS.
Abbreviations: NMR, nuclear magnetic resonance; TPGS, d-α-tocopherol polyethylene glycol 1000 succinate.

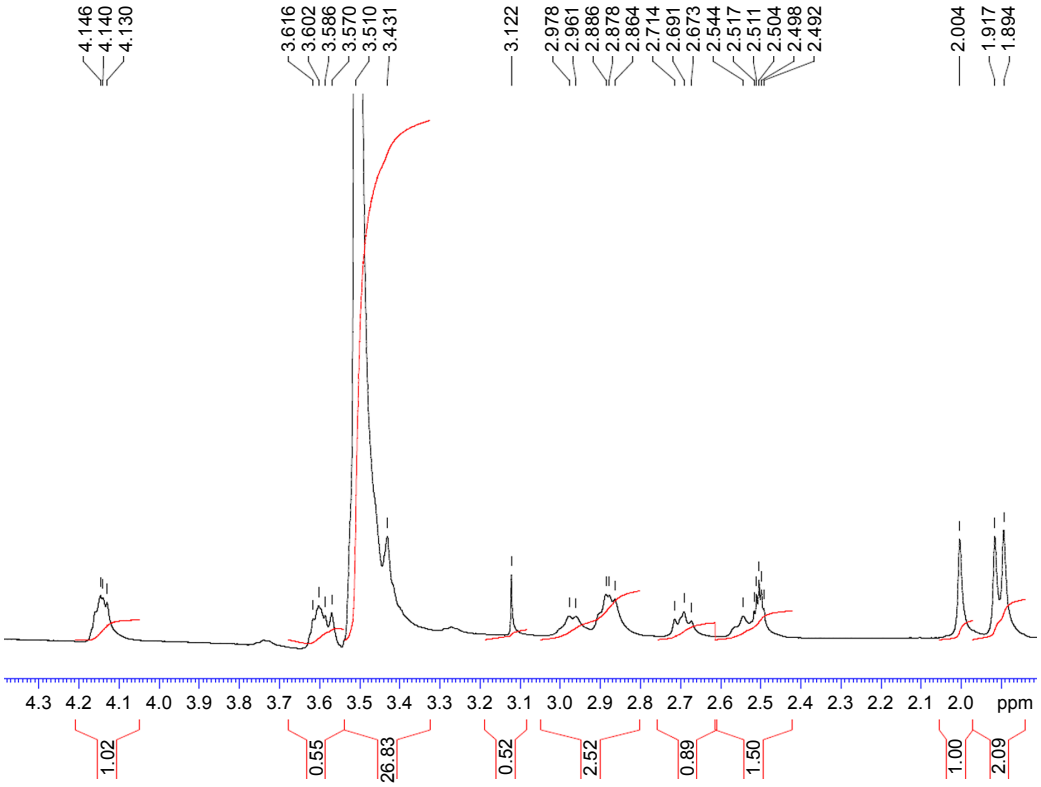

Figure S3 ^{1}H NMR spectrum (2–4.4 ppm) of TPGS.
Abbreviations: NMR, nuclear magnetic resonance; TPGS, d-α-tocopherol polyethylene glycol 1000 succinate.

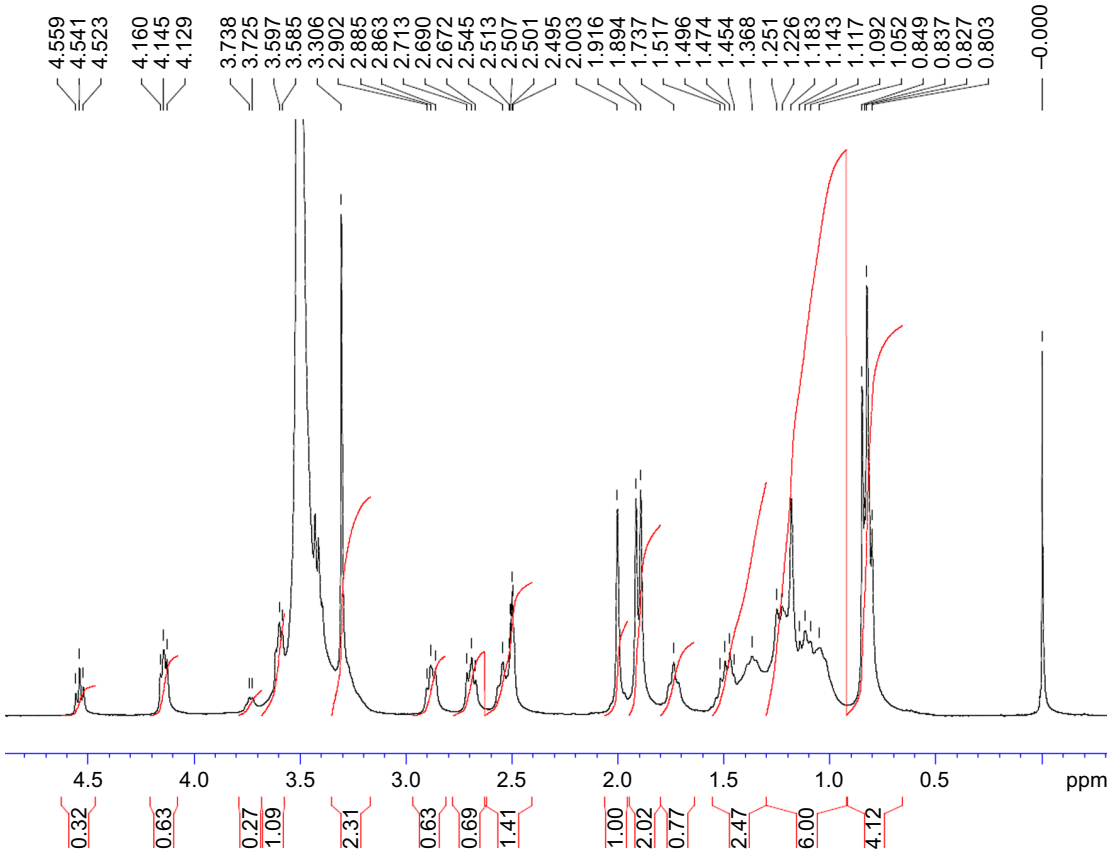

Figure S4 ^{1}H NMR spectrum (0–5 ppm) of synthesized TPGS-DTPA.
Abbreviations: NMR, nuclear magnetic resonance; TPGS-DTPA, d-α-tocopherol polyethylene glycol 1000 succinate-diethylenetriaminepentaacetic acid.

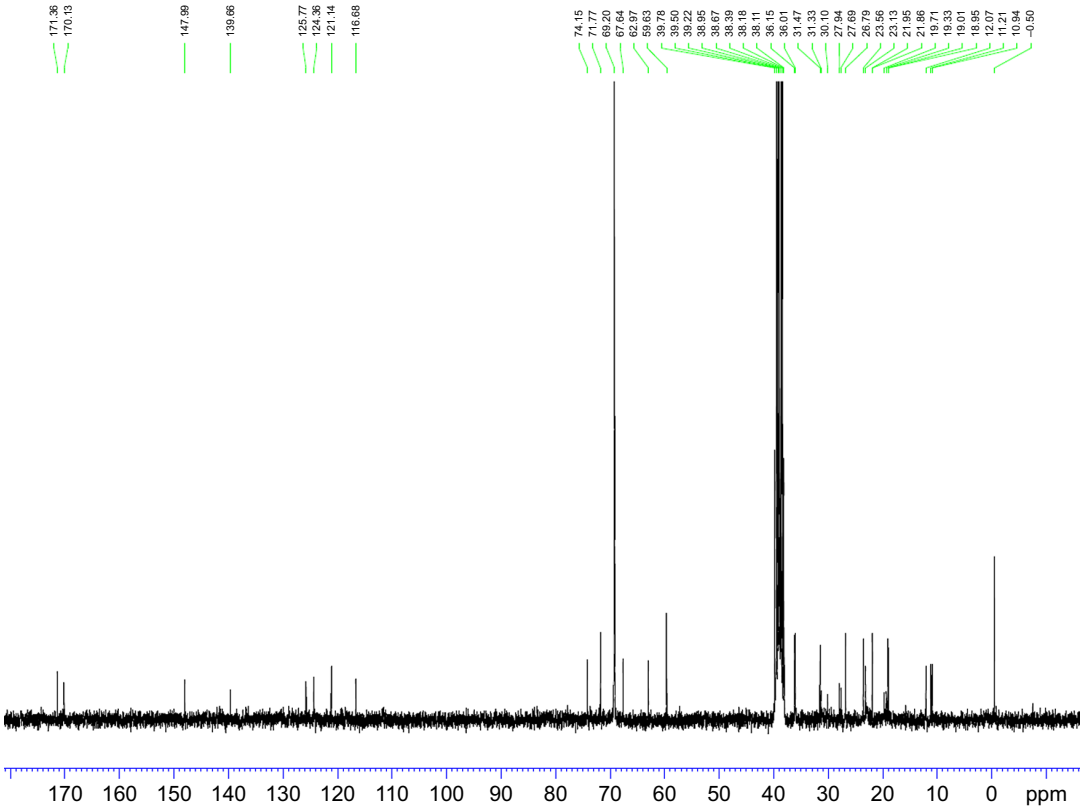

Figure S5 ^{13}C NMR spectrum (0–180 ppm) of TPGS.
Abbreviations: NMR, nuclear magnetic resonance; TPGS, d-α-tocopherol polyethylene glycol 1000 succinate.

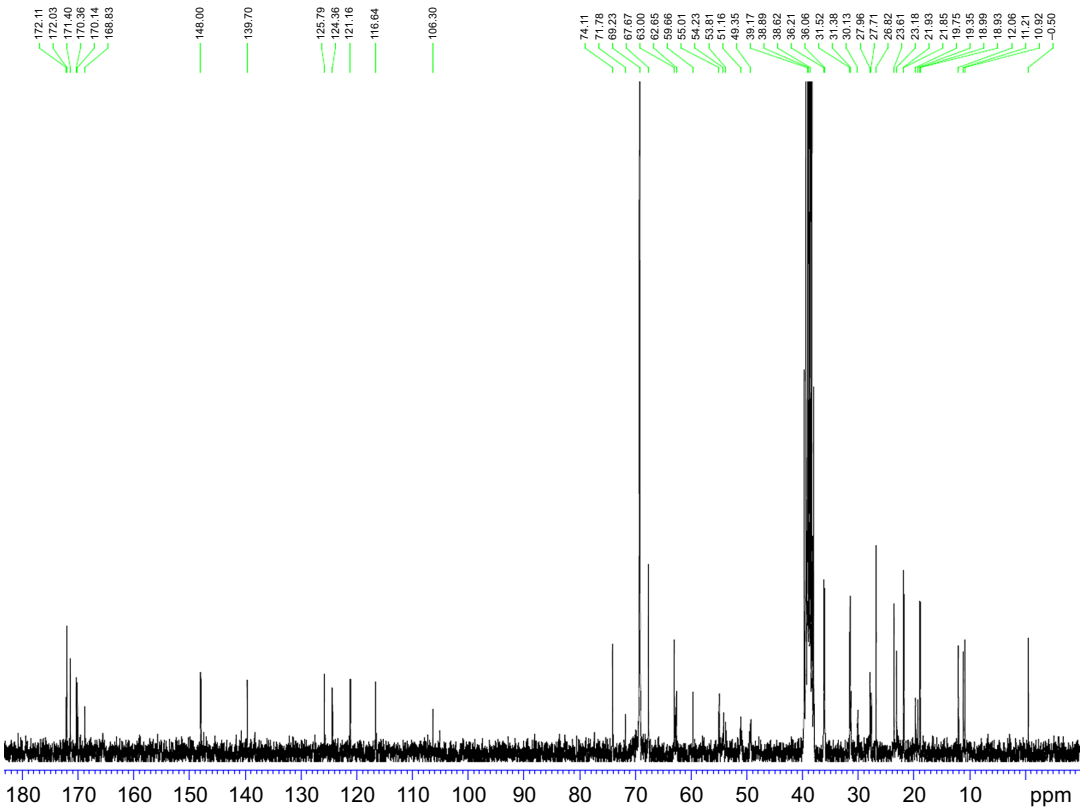

Figure S6 ^{13}C NMR spectrum (0–180 ppm) of synthesized TPGS-DTPA.
Abbreviations: NMR, nuclear magnetic resonance; TPGS-DTPA, d-α-tocopherol polyethylene glycol 1000 succinate-diethylenetriaminepentaacetic acid.

Table S1 Effect of increasing probe sonication times on particle size and PDI of niosomes (N3)

Sonication time (minute)	Particle size (nm)	PDI
0	610.1±111.3	0.741±0.111
2	389.2±62.7	0.610±0.129
4	221.2±21.5	0.523±0.109
8	124.8±6.8	0.294±0.076
12	130.8±3.1	0.241±0.031

Abbreviation: PDI, polydispersity index.

Table S2 The effect of temperature on radiolabeling efficiency

Temperature (°C)	$^{99m}TcO_4^-$ (%)	Radiocolloids (%)	^{99m}Tc-labeled niosomes (%)	Loaded amount of ^{99m}Tc (mCi)
23	1.36±0.37	1.70±0.31	96.94±0.61	1.94±0.01
37	2.30±0.36	1.44±0.14	96.26±0.48	1.93±0.01

Notes: Formulation N3: $SnCl_2 \cdot H_2O$ 30 μg/mL; pH 5; and incubation time 15 min.
Abbreviations: $SnCl_2 \cdot H_2O$, stannous chloride; ^{99m}Tc, Technetium-99m.

Table S3 Effect of increasing probe sonication times on particle size and PDI of niosomes (N3)

Niosomes	Particle size (nm)	PDI	Zeta potential (mV)
Blank	129.1±3.7	0.193±0.011	−68.6±2.9
T3-loaded (15 mg/mL)	127.3±1.5	0.218±0.013	−67.2±3.6

Abbreviation: PDI, polydispersity index.